



FRAGILITY FUNCTIONS OF BUILDINGS UNDER ONLY TSUNAMI LOAD IN INDONESIA: A CASE STUDY OF THE 2018 SUNDA STRAIT TSUNAMI

A. Suppasri⁽¹⁾, K. Pakoksung⁽²⁾, Syamsidik⁽³⁾, P. Latcharote⁽⁴⁾, R. Miyamoto⁽⁵⁾, F. Imamura⁽⁶⁾

⁽¹⁾ Associate Professor, International Research Institute of Disaster Science, Tohoku University, suppasri@irides.tohoku.ac.jp

⁽²⁾ Postdoctoral Fellow, International Research Institute of Disaster Science, Tohoku University, pakoksung@irides.tohoku.ac.jp

⁽³⁾ Lecturer, Tsunami and Disaster Mitigation Research Center (TDMRC), Universitas Syiah Kuala, Banda Aceh, Indonesia., syamsidik@tdmrc.org

⁽⁴⁾ Lecturer, Department of Civil and Environmental Engineering, Faculty of Engineering, Mahidol University, panon.lat@mahidol.ac.th

⁽⁵⁾ Research Associate, International Research Institute of Disaster Science, Tohoku University, rmiyamoto@irides.tohoku.ac.jp

⁽⁶⁾ Professor, International Research Institute of Disaster Science, Tohoku University, imamura@irides.tohoku.ac.jp

Abstract

Most of previously developed tsunami fragility functions in many countries used building damage data from local tsunamis. Similar to Indonesia which experienced many tsunamis and some tsunami fragility functions were developed. However, all of them are influenced by earthquake. The 2018 Sunda Strait tsunami was generated by the collapsed of Anak Krakatoa volcano. Therefore, damaged buildings by this tsunami were only caused by tsunami load. This study performed numerical simulation (TUNAMI two-layer model) with nesting grid system using the finest grid size of 20 m to reproduce hydrodynamic parameters of tsunami and verified by measured tsunami trace and actual inundation area. There are several field surveys conducted for this tsunami including preliminary developed tsunami fragility functions using measured maximum flow depth. Simulation results (maximum flow depth, maximum flow velocity and maximum hydrodynamic force) were combined with damaged building data and developed tsunami fragility functions using linear regression analysis for the 2018 Sunda Strait tsunami. It can be seen that more than half of the buildings could withstand 4 m flow depth. In addition, comparison of fragility functions of damaged buildings caused by the 2018 Sunda Strait and the 2004 Indian Ocean tsunami in Banda Aceh shows that damaged buildings in Banda Aceh had higher damage probability (at the same flow depth) than damaged buildings around the Sunda Strait tsunami affected area. This is because it was only short period tsunami for the 2018 tsunami but combination of considerable ground motion (MMI 7.5), long period tsunami as well as debris impact for the 2004 tsunami. This is the first attempt in quantitatively demonstrated such integrated impact on building damage in terms of the fragility functions which will be useful when assessing building damage in the future against different types of tsunamis.

Keywords: 2018 Sunda Strait tsunami, tsunami load, fragility functions, building damage assessment



1. Introduction

The 2018 Sunda Strait tsunami occurred on December 22, 2018. It was the second landslide tsunami in Indonesia in the instrumental generation after the 2018 Sulawesi tsunami that occurred in September 2018. This 2018 Sunda Strait tsunami was generated by mass failures caused by volcanic eruption of the Anak Krakatau volcano in Sunda Strait, Indonesia. The tsunami killed 437 lives and few thousands buildings [1]. At present, there are many previously published works on tsunami fragility functions based on damaged data from past tsunamis in Indonesia; the 2004 Indian Ocean tsunami [2], the 2006 Java tsunami [3] and other countries; the 2004 Indian Ocean tsunami in Thailand [4], in Sri Lanka [5], 2009 American Samoa [6], 2010 Chile [7] and 2011 Great East Japan tsunami [8]. These fragility functions were developed over the world with different engineering practice and construction technique but the same earthquake generated tsunamis. Earthquake generated tsunamis normally have long wave periods (in order of an hour) due to their fault width. On the other hand, landslide tsunamis have much shorter wave period. The dominant wave period of the 2018 Sunda Strait is approximately 7 min [1]. It is expected that earthquake generated tsunamis cause larger damage than landslide tsunamis because 1) ground shaking caused by earthquake, 2) liquefaction caused by earthquake and 3) wave attacking period during tsunami inundation is much longer. All previous developed fragility functions were not only tsunami force but were influenced by ground shaking and/or liquefaction. Nevertheless, this 2018 Sunda Strait was the first event of purely tsunami force acting on buildings. Therefore, this study has main objective to investigate relationship between only tsunami force and building damage using results from tsunami simulation and damaged building data from field survey.

2. Data and method

2.1 Tsunami flow depth data and damaged building data

As shown in Fig. 1, tsunami flow depths measured at buildings and other traces [9] were used for validation of the tsunami simulation results. There are 130 points of tsunami trace and 98 flow depths at damaged buildings. The maximum surveyed flow depth is 6.6 m.

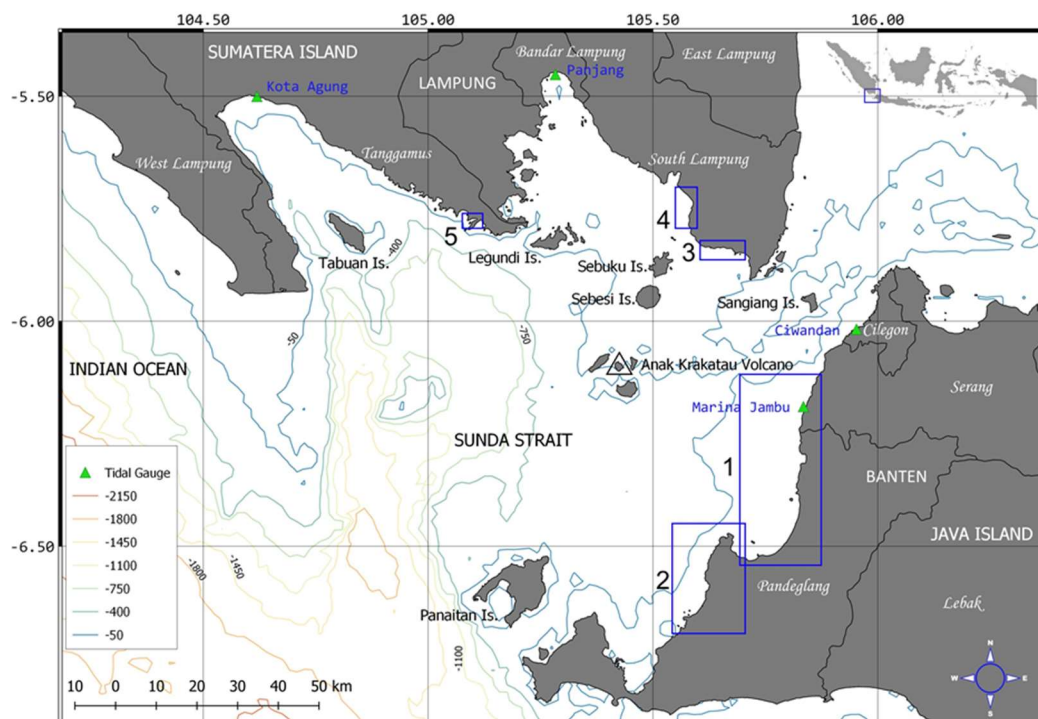







Fig. 1 – Five tsunami trace and damaged building surveyed area of the 2018 Sunda Strait tsunami as shown in blue rectangles [9]



Most of houses in this area were made confined masonry infill bricks wall type houses (CM type). The types of the houses were similar to those in Banda Aceh before the 2004 Indian Ocean tsunami. A significant difference was identified on roof materials of the houses. In Sunda Strait area, a number of houses used tiles-roof. Meanwhile in Banda Aceh, majority of houses used zinc-plate roof. Despite the roof material, other components of the houses at both of the tsunami-affected areas were similar and this made the two cases are comparable. Among the 98 damaged buildings, there are 68 confined masonry concrete houses, 27 wooden houses and 3 others. The damaged were classified in four levels, Level 1: Minor damage, Level 2: Moderate damage, Level 3: Major damage and Level 4: Complete damage or washed away as shown in Table 1. As preliminary study, confined masonry concrete houses were combined with wooden houses for further development of fragility functions. A reason for combining the two building types is because fragility functions of the 2004 Indian Ocean tsunami were also developed using mixed building types as they were interpreted from satellite images before and after the tsunami.

Table 2 –Damage levels and their descriptions from the field survey [9]

Damage level	Damage level	Descriptions	Example photos
0	No damage	Flooded but no damages found.	
1	Minor	Damages found windows and doors, no damage on wall and on structural component	
2	Moderate	One side wall damages, no damage on column and beam.	
3	Major	All walls were damaged or roofs felt down, structural components bent/deflected or broken.	
4	Complete washed away or	Only floor left.	



2.2 Tsunami numerical simulation

Nonlinear shallow-water equation with partial differential equations TUNAMI was used together with a two-layer model that considered two interfacing layers and appropriate kinematic and dynamic boundary conditions at the seafloor, interface, and water surface [10]. This two-layer numerical model simulates landslide-generated tsunamis by modeling the interactions between tsunami generation and submarine landslides as upper and lower layers. In recent years, the two-layer model has been improved and widely implemented in tsunami hazard assessment around the world [11,12] and applied to a similar problem in case of the 2018 Sulawesi tsunami [13]. The basic assumption of a subaerial/submarine landslide tsunami was estimated using the landslide volume of 0.142 km^3 based on satellite images before and after the eruption together with other simulation conditions [14].

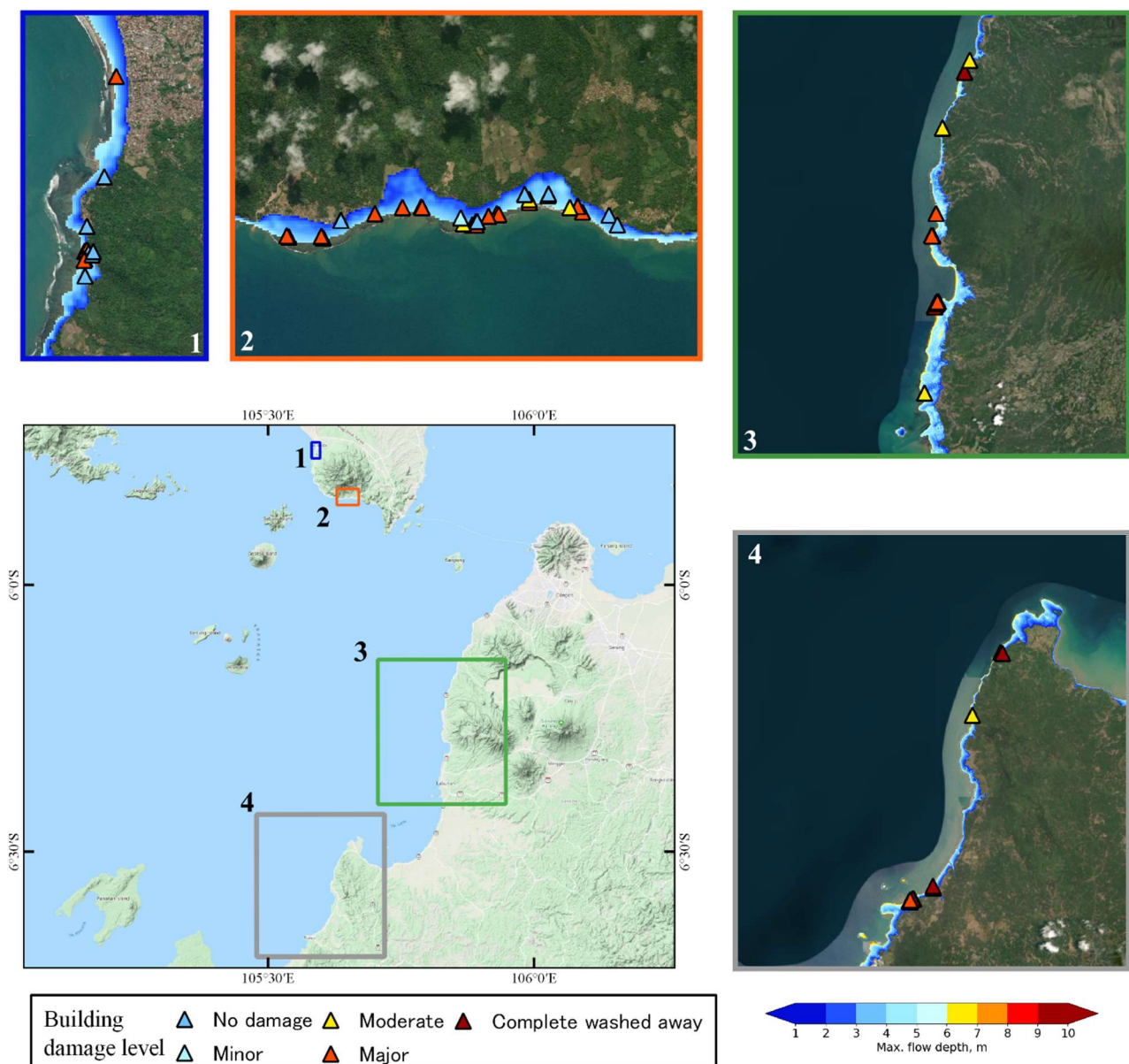


Fig. 2 –Tsunami simulation result that show the simulated maximum flow depth and inundation area overlaying on the damaged building data



3. Results

3.1 Validation of tsunami simulation results

Validation of the computed waveforms is performed using the parameters K and κ proposed [15], as defined below:

$$\log K = \frac{1}{n} \sum_{i=1}^n \log K_i \quad (1)$$

$$\log \kappa = \sqrt{\frac{1}{n} \sum_{i=1}^n (\log K_i)^2 - (\log K)^2} \quad (2)$$

$$K_i = \frac{x_i}{y_i} \quad (3)$$

Therein, x_i and y_i are the surveyed and computed maximum tsunami flow depth at location i . Thus, K is defined as the geometrical mean of K_i and κ is defined as deviation or variance from K . These indices are used as criteria to validate the model through the comparison between the simulated and surveyed tsunamis. Fig. 3 shows comparison of the simulated and surveyed maximum flow depths at tsunami trace points in Fig. 3(a) and at damaged buildings in Fig. 3(b). Although the K and κ values of the trace points ($K = 0.72$ and $k = 1.74$) is not that good but K and κ values of the damaged buildings is acceptable ($K = 0.84$ and $k = 1.71$). The simulated maximum flow depth, maximum flow velocity and maximum hydrodynamic force were then used for further developing of fragility functions in the next section.

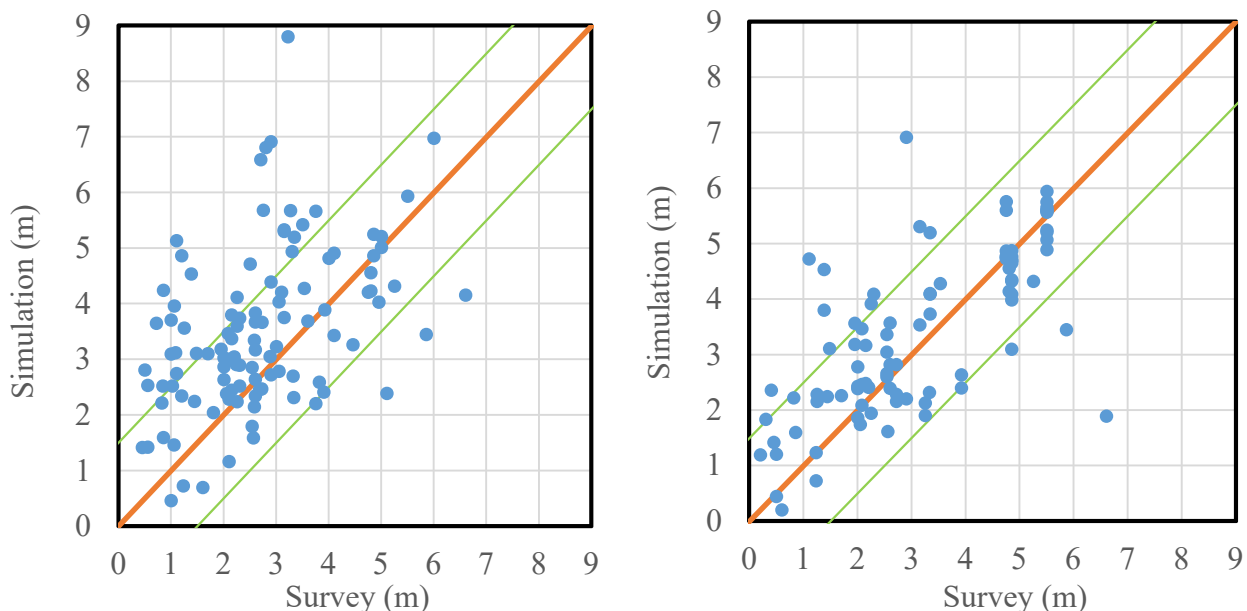


Fig. 3 –Comparisons of simulation results and surveyed flow depths (a) Tsunami trace and (b) Damaged buildings



3.2 Developing tsunami fragility functions

From the damaged building data, a histogram of tsunami features (flow depth, flow velocity, and hydrodynamic force) and the number of buildings including the ones not damaged and the ones damaged (damage levels 2, 3 and 4) is plotted. The damage probabilities of buildings and a discrete set were calculated and shown against a median value. Linear regression analysis was performed to develop the fragility function. The cumulative probability P of occurrence of damage is given either by Eq. (4) or by (5):

$$P(x) = \Phi \left[\frac{x - \mu}{\sigma} \right] \quad (4)$$

$$P(x) = \Phi \left[\frac{\ln x - \mu'}{\sigma'} \right] \quad (5)$$

In these equations, Φ represents the standardized normal (lognormal) distribution function, x stands for the hydrodynamic feature of tsunami (e.g., inundation depth, current velocity and hydrodynamic force), and μ and σ (μ' and σ') respectively signify the mean and standard deviation of x ($\ln x$). Two statistical parameters of fragility function, μ and σ (μ' and σ'), are obtained by plotting x ($\ln x$) against the inverse of Φ on normal or lognormal probability papers, and performing least-squares fitting of this plot. Consequently, two parameters are obtained by taking the intercept ($= \mu$ or μ') and the angular coefficient ($= \sigma$ or σ') in Eq. (6) or (7):

$$x = \sigma \Phi^{-1} + \mu \quad (6)$$

$$\ln x = \sigma' \Phi^{-1} + \mu' \quad (7)$$

Throughout the regression analysis, the parameters are determined as shown in Table 2 to obtain the best fit of fragility curves with respect to the flow depth (Fig. 4(a)), the flow velocity (Fig. 5(a)) and the hydrodynamic force on structures per unit width (Fig. 6(a)).

Table 2 –Parameters for tsunami fragility functions as functions of the maximum flow depth, maximum flow velocity and maximum hydrodynamic force

X for fragility function $P(x)$	μ	σ	μ'	σ'	R^2
Flow depth: Damage level 2	1.6395	0.5172			0.7792
Flow depth: Damage level 3	2.3449	1.3364			0.8421
Flow depth: Damage level 4	4.2748	1.1392			0.7424
Flow velocity: Damage level 2			0.7556	0.3661	0.8537
Flow velocity: Damage level 3			1.0767	0.5567	0.7853
Flow velocity: Damage level 4			1.9267	0.4756	0.7728
Hydrodynamic force: Damage level 2			1.366	1.0364	0.8460
Hydrodynamic force: Damage level 3			2.1944	1.6316	0.8753
Hydrodynamic force: Damage level 4			4.5531	1.3983	0.8347

The hydrodynamic force acting on a structure is defined as its drag force per unit width, as

$$F = \frac{1}{2} C_D \rho u^2 D, \quad (8)$$



where C_D denotes the drag coefficient ($C_D = 1.0$ [Koshimura 2009]), ρ is the density of water ($= 1,000 \text{ kg/m}^3$), u stands for the current velocity (m/s), and D is the inundation depth (m). From this result, the fragility functions with respect to the flow depth, is given by the standardized lognormal distribution functions with μ and σ where as flow velocity and hydrodynamic force are given by the standardized lognormal distribution functions with μ' and σ' . Similarly, comparison of fragility functions for damage level 4 of the 2018 Sunda Strait tsunami were compared with the 2004 Indian Ocean tsunami in Banda Aceh [2] as shown in Figs. 4(b), 5(b) and 6(b) for maximum flow depth, maximum flow velocity and maximum hydrodynamic force respectively.

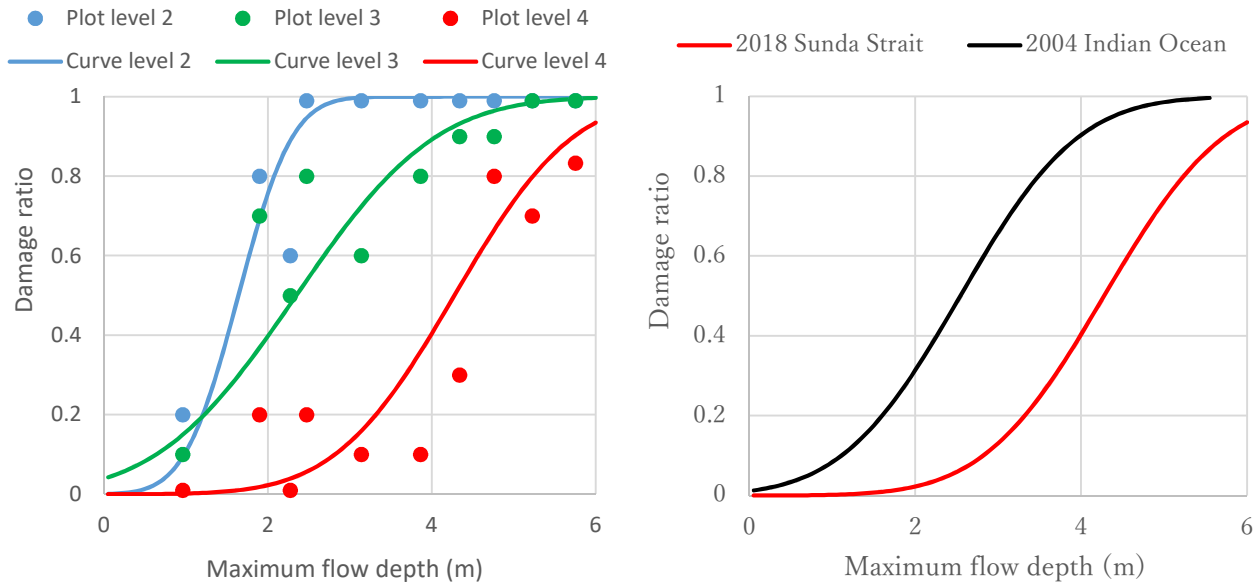


Fig. 4 –Fragility functions as a function of maximum flow depth (a) Fragility functions for four damage levels 2, 3 and 4 of the 2018 Sunda Strait tsunami and (b) Comparison of fragility functions of the 2018 Sunda Strait tsunami (damage level 4) and the 2004 Indian Ocean tsunami [2]

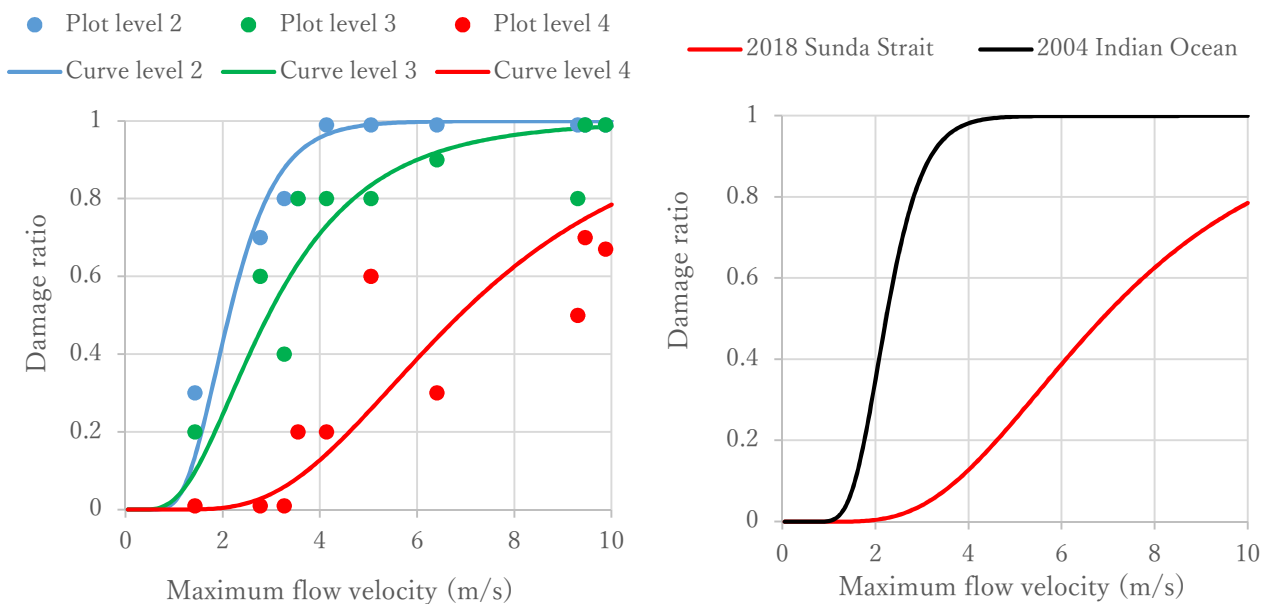


Fig. 5 –Fragility functions as a function of maximum flow velocity (a) Fragility functions for four damage levels 2, 3 and 4 of the 2018 Sunda Strait tsunami and (b) Comparison of fragility functions of the 2018 Sunda Strait tsunami (damage level 4) and the 2004 Indian Ocean tsunami [2]

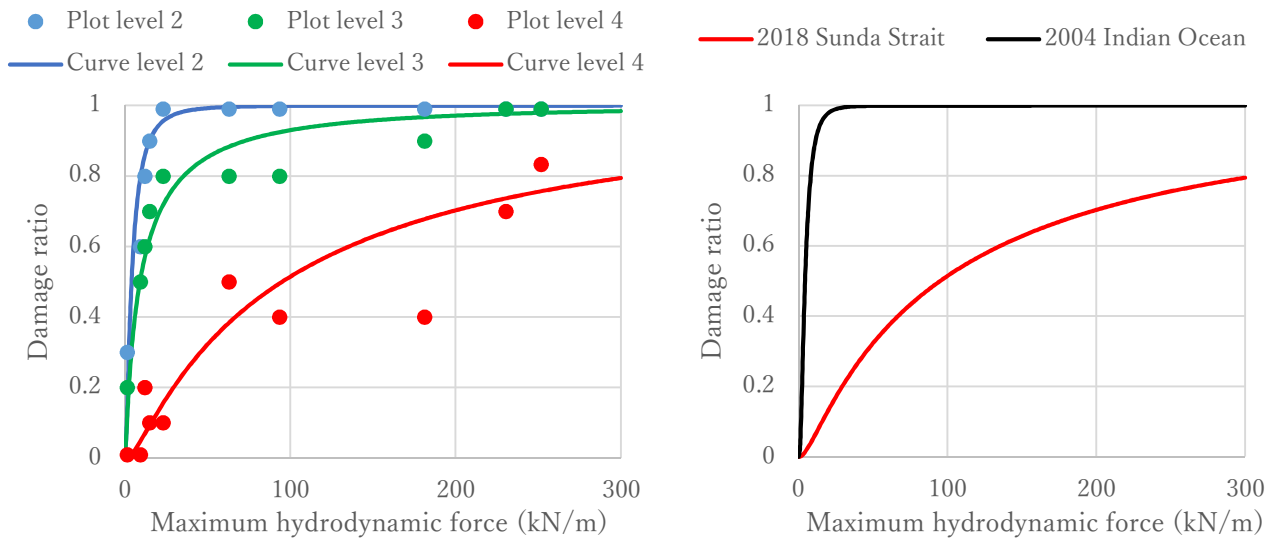


Fig. 6 –Fragility functions as a function of maximum hydrodynamic force (a) Fragility functions for four damage levels 2, 3 and 4 of the 2018 Sunda Strait tsunami and (b) Comparison of fragility functions of the 2018 Sunda Strait tsunami (damage level 4) and the 2004 Indian Ocean tsunami [2]

4. Discussions

Damage level 4 (complete damage or washed away) of the 2018 Sunda Strait was used to compared with damage classified by satellite images (roofs remaining or not) of the 2004 Indian Ocean tsunami [2] when comparing fragility functions of the two tsunami events. The comparison gives very clear understanding of disaster characteristics input and building damage as output. Maximum flow depth of 2 m has been using as damage criteria based on results of the 2004 tsunami. However, most buildings could withstand 2 m flow depth in case of the 2018 tsunami as shown in Fig. 4(b). Similar trend can be seen with the comparisons using maximum flow velocity and maximum hydrodynamic force as shown in Figs 5(b) and 6(b). These results clearly demonstrated that impacts from ground shaking as well as long wave period induced larger damage to buildings. Further discussion can be made in the future when comparing these two tsunami events with the 2018 Sulawesi tsunami to demonstrate impact from liquefaction.

5. Conclusions

This study reproduced the 2018 Sunda Strait tsunami using numerical where simulation results were validated using surveyed flow depths data with acceptable range of reliability. Damaged building data of both confined masonry concrete buildings and wooden houses of 96 buildings classified in four damage levels were used. The tsunami numerical simulation results (maximum flow depth, maximum flow velocity and maximum hydrodynamic force) were combined with damaged building data using linear regression analysis for developing fragility functions of the 2018 Sunda Strait tsunami. It is clearly demonstrated that more than half of the buildings could withstand against maximum tsunami flow depth of 4 m. The comparison with the 2004 Indian Ocean tsunami with largely influenced by strong ground shaking and much longer wave period shows that such impacts are much contributed to enlarge the building damage. This is the first time that such impact is quantitatively presented. There are still some points that shall be improved in the future. For example, overlapping of the curves in Fig. 3(a) can be improved by increasing tsunami simulation accuracy, separating building material types as well as applying more advanced statistical method.

6. Acknowledgements

This research was funded and supported by the Core Research Cluster of Disaster Science in Tohoku University (Designated National University), Tokio Marine & Nichido Fire Insurance Co., Ltd., Willis



Research Network (WRN), Pacific Consultants Co., LTD and the World Class Professor Program (WCP) Scheme B, promoted by Ministry of Research, Technology, and Higher Education of Indonesia (KEMENRISTEKDIKTI) in 2019 (Contract No. T/80/D2.3/KK.04.05/2019).

7. References

- [1] Muhari A, Heidarzadeh M, Susmoro H, Nugroho HD, Kriswati E, Supartoyo Wijanarto AB, Imamura F, Arikawa T (2019): The December 2018 Anak Krakatau volcano tsunami as inferred from post-tsunami field surveys and spectral analysis, *Pure and Applied Geophysics*, **176**, 5219.
- [2] Koshimura S, Oie T, Yanagisawa H, Imamura F (2009): Developing fragility curves for tsunami damage estimation using numerical model and post-tsunami data from Banda Aceh, Indonesia, *Coastal Engineering Journal*, **51**, 243–273.
- [3] Reese S, Cousins WJ, Power WL, Palmer NG, Tejakusuma IG, Nugrahadi S (2007): Tsunami vulnerability of buildings and people in South Java – Field observations after the July 2006 Java tsunami, *Natural Hazards and Earth System Sciences*, **7**, 573–589.
- [4] Suppasri A, Koshimura S, Imamura F. (2011): Developing tsunami fragility curves based on the satellite remote sensing and the numerical modeling of the 2004 Indian Ocean tsunami in Thailand, *Natural Hazards and Earth System Sciences*, **11**, 173–189.
- [5] Leelawat N, Suppasri A, Murao O, Imamura F (2016): A study on the influential factors on building damage in Sri Lanka from the 2004 Indian Ocean tsunami, *Journal of Earthquake and Tsunami*, **10** (2), 1640001.
- [6] Gokon H, Koshimura S, Imai K, Matsuoka M, Namegaya Y, Nishimura Y (2014): Developing fragility functions for the areas affected by the 2009 Samoa earthquake and tsunami, *Natural Hazards and Earth System Sciences*, **14**, 3231–3241.
- [7] Mas E, Koshimura S, Suppasri A, Matsuoka M, Yoshii T, Jimenez C, Yamazaki F, Imamura F (2012): Developing tsunami fragility curves using remote sensing and survey data of the 2010 Chilean tsunami in Dichato, *Natural Hazards and Earth System Sciences*, **12** (8), 2709–2718.
- [8] Suppasri A, Charvet I, Imai K, Imamura F (2015): Fragility curves based on data from the 2011 Great East Japan tsunami in Ishinomaki city with discussion of parameters influencing building damage, *Earthquake Spectra*, **31** (2), 841–868.
- [9] Syamsidik, Benazir, Luthfi M, Suppasri A, Comfort LK (2020): The 22 December 2018 Mount Anak Krakatau Volcanogenic Tsunami on Sunda Strait Coasts, Indonesia: tsunami and damage characteristics, *Natural Hazards and Earth System Sciences* (Accepted) Available at: <http://doi.org/10.5194/nhess-2019-252>.
- [10] Imamura F, Imteaz MA (1995): Long waves in two-layers: Governing equations and numerical model, *Science of Tsunami Hazards*, **13**(1), 3–24.
- [11] Latcharote, P, Suppasri, A, Imamura, F, Aytore, B, Yalciner, AC (2016): Possible Worst-Case Tsunami Scenarios around the Marmara Sea from Combined Earthquake and Landslide Sources, *Pure and Applied Geophysics*, **173**(12), 3823–3846.
- [12] Latcharote, P, Al-Salem, K, Suppasri, A, Pokavanich, T, Toda, S, Jayaramu, Y, Al-Enezi, A, AlRagum, A, Imamura, F (2018): Tsunami Hazard Evaluation for Kuwait and Arabian Gulf Due to Makran Subduction Zone and Subaerial Landslides. *Natural Hazards*, **93**(sp.1), 127–152.
- [13] Pakogsung K, Suppasri A, Imamura F, Athanasius C, Omang A, Muhari A (2019): Simulation of the submarine landslide tsunami on 28 September 2018 in Palu Bay, Sulawesi Island, Indonesia, using a two-layer model, *Pure and Applied Geophysics*, **176** (8), 3323–3350.
- [14] Pakogsung K, Suppasri A, Muhari A, Syamsidik, Imamura F (2020): Global optimization of numerical two-layer model using observed data: A case study of the 2018 Sunda Straits tsunami, in *proceedings of the 17th World Conference on Earthquake Engineering*, Sendai, Japan, 13–18 September 2020.
- [15] Aida I (1978): Reliability of a tsunami source model derived from fault parameters, *Journal of Physics of Earth*, **26**, 57–73.